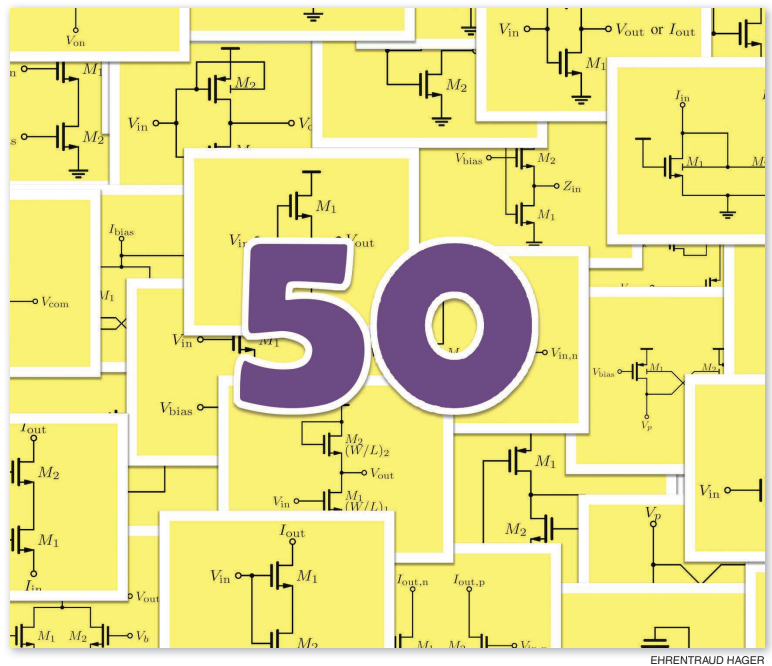


# Fifty Nifty Variations of Two-Transistor Circuits



*A tribute to the versatility of MOSFETs*

**W**e present a compendium of two-metal-oxide-semiconductor (MOS)-transistor circuits, which span the range from simple standard configurations to ingenious arrangements. Using these building blocks, circuit designers can assemble a vast array of complex analog functions. This (incomplete) collection shall serve as a reference and inspiration to junior circuit designers and hopefully contains at least one unexpected example for professional engineers.

## Overview

Analog circuit design is wonderfully creative. The MOS field-effect transis-

tor (MOSFET) is an exceptionally versatile device, operating as a switch, current source, resistor, diode, and capacitor, depending on bias conditions. For fun and to demonstrate the sheer infinite possibilities in circuit design using MOSFET, we present a collection of simple (and sophisticated) circuits that employ two transistors (not counting fixed-bias and supply voltages and fixed-bias currents). Often, circuit designers construct complex circuits from these basic building blocks.

This compendium is a tribute to all of the ingenious minds out there and the circuit design giants on whose shoulders we are standing today. This sample of practical two-transistor circuits, to the best of the authors' knowledge, contains beneficial and often-used configurations. A few circuits are of a more curious and academic nature; they might lack

power-supply rejection or show other deficiencies, and some circuits use the body connection as active terminals, which might not be feasible in some CMOS technologies. Generally, one has to be aware of the body effect and its impact.

Many more two-transistor circuits are yet to be discovered. An exhaustive search of graphs using one or two voltage-controlled current sources (which are well-approximated by MOSFET) resulted in 150 potentially useful circuits [1]. One of them was identified as a valuable new amplifier configuration [2]. By pushing this idea further, a study identified 582 possible circuit topologies using two transistors. Repeating this exercise using three transistors, a whopping 56,280 elementary configurations have been found [3].

To keep our overview reasonable, we do not include complementary

Digital Object Identifier 10.1109/MSSC.2021.3088968  
Date of current version: 25 August 2021

circuits that can be constructed by swapping n-MOSFET (NMOS) for p-MOSFET (PMOS) devices (or vice versa).

### Logic Circuits

First, we present simple circuits that operate on logical inputs, like the inverter (Figure 1), and an improved low-voltage version that exploits the body terminals in a DTMOS inverter (Figure 2). Terminating an unused input of a logic gate to a logical one or zero, an ESD-safe tie-zero or tie-one, respectively, should be utilized, like the one presented in Figure 3. Using the unusual arrangement in Figure 4, we can implement an XNOR logic function while the implementations of NAND and NOR as presented in Figures 5 and 6, respectively, are the fundamental building blocks of the digital universe.

### Basic Circuits

This section presents the basic circuits constituting the fundamental building blocks of the analog and mixed-signal

**This (incomplete) collection shall serve as a reference and inspiration to junior circuit designers and hopefully contains at least one unexpected example for professional engineers.**

world, like the current mirror displayed in Figure 7. The differential pair (Figure 8) is constructed alternatively with

or without a tail current source, which is often called a *pseudodifferential pair*. The source follower in Figure 9 is one

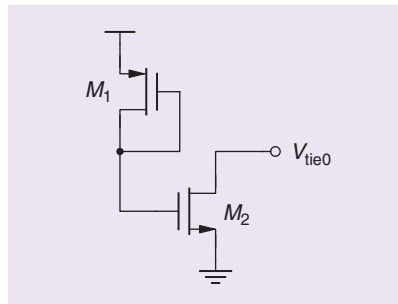


**FIGURE 3:** An electrostatic discharge (ESD)-safe tie-zero for unused CMOS logic inputs (no MOSFET gate is tied directly to a supply rail). The tie-one can be constructed accordingly.

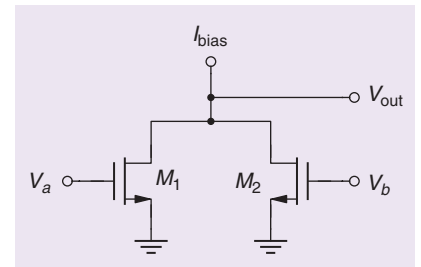


**FIGURE 6:** This circuit complements the logic gates implemented in Figures 4 and 5 and realizes a NOR function ( $V_{out} = \overline{V_a \vee V_b}$ ).

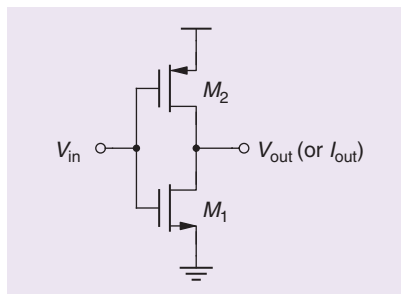


**FIGURE 1:** The ubiquitous digital inverter. The input voltage  $V_{in}$  switches one of the transistors on while the other is off [4].

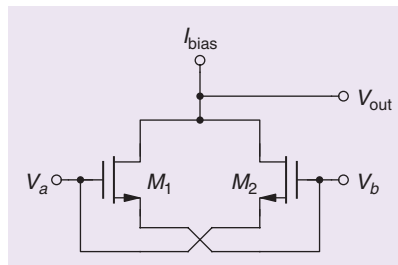


**FIGURE 4:** Using a current source  $I_{bias}$  with finite output impedance to bias this structure, this circuit implements an XNOR logic function ( $V_{out} = \overline{V_a \oplus V_b}$ ). The logic inputs  $V_a$  and  $V_b$  must be driven by low-ohmic logic levels between  $V_{DD}$  and  $V_{SS}$  [6].

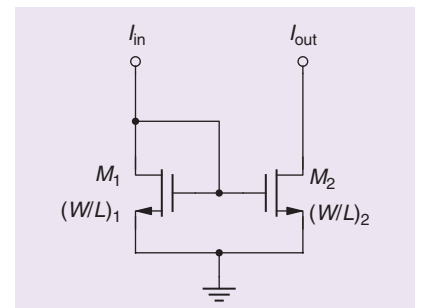


**FIGURE 7:** The basic current mirror achieves a simultaneous copying and sizing of  $I_{out} = (W/L)_2 / (W/L)_1 \cdot I_{in}$  according to the dimensions of  $M_1$  and  $M_2$  [7].

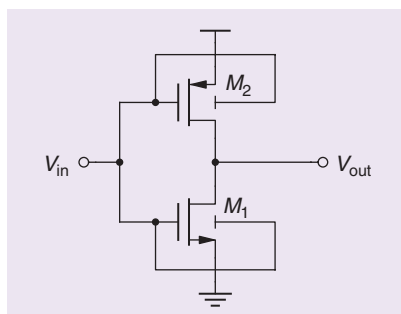


**FIGURE 2:** The dynamic-threshold-voltage MOSFET (DTMOS) inverter achieves an improved current drive at low-leakage current. It needs to be operated at low supply voltages to avoid a forward bias of the well diodes [5].

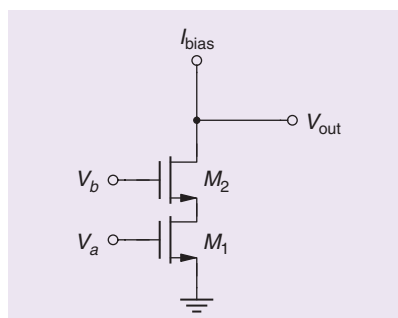


**FIGURE 5:** This series connection of two MOSFETs realizes a logical NAND function ( $V_{out} = \overline{V_a \wedge V_b}$ ).

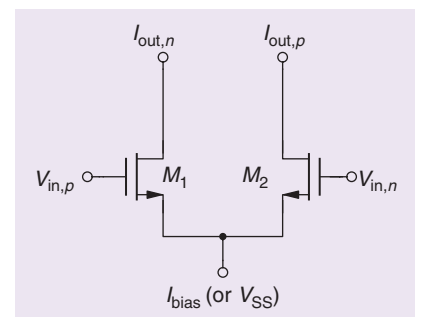


**FIGURE 8:** The ubiquitous differential pair, like the current mirror in Figure 7, is a fundamental building block in integrated circuits [8]. The pseudodifferential variant spares the tail current source's headroom in exchange for reduced common-mode rejection but with the benefit of class-AB action.

## The generation of a bias voltage is a task that is often encountered in analog circuit design.

of the elementary circuits that is useful in many situations, just like the common-source amplifier with active load (Figure 10). Adding a cascode to a circuit is a powerful technique. For example, a common-gate combined with a common-source stage is depicted in Figure 11, and the cascade of two common-gate stages is illustrated in Figure 12. Of course, the essential common-gate stage qualifies as a two-transistor circuit as well (Figure 13).

The transmission gate (Figure 14) is an essential building block, allowing switching voltages and currents (a feat making the MOSFET such a valuable device). With a straightforward extension, a multiplexer can be constructed (Figure 15). However, in most practical implementations, a set of transmission gates will be applied for this purpose.

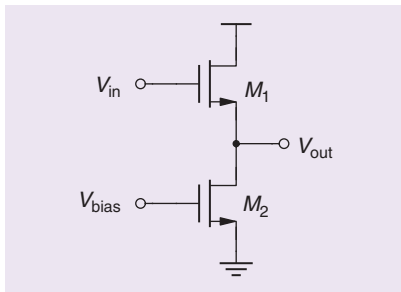


**FIGURE 9:** The source follower (or common-drain stage) utilizing  $M_2$  as a current source to bias  $M_1$ .

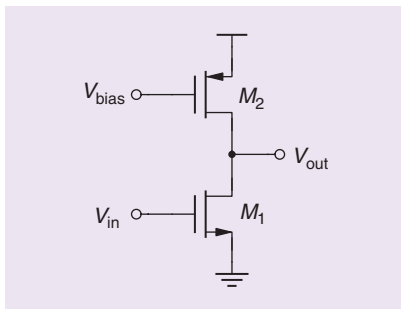


**FIGURE 10:** The common-source amplifier with active load.

### Improved Basic Circuits

It has been realized that the digital inverter presented in Figure 1 can

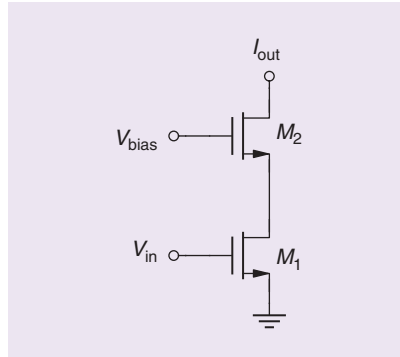


**FIGURE 11:** The cascoded common-source stage boosting the output impedance of  $M_1$  considerably to  $r_{out} \approx g_{m2}/(g_{ds1} \cdot g_{ds2})$ .

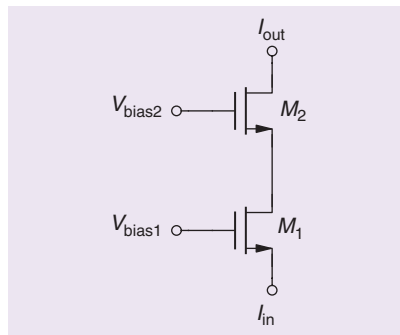


**FIGURE 12:** The cascoded common-gate stage. Note that  $I_{out} \approx I_{in}$ , but the impedance level changes drastically, creating gain or a high output impedance at the output node.

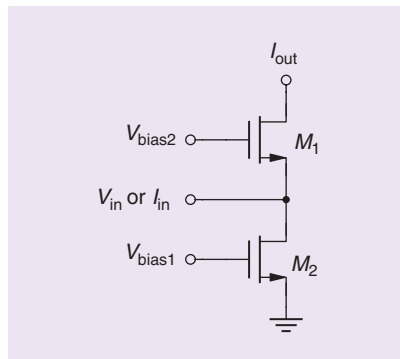


**FIGURE 13:** The common-gate stage employing  $M_2$  as a current source to the bias transistor  $M_1$ .

also be employed as an excellent low-voltage amplifier ( $V_{out}$ ) or trans-conductance stage ( $I_{out}$ ) when both transistors are biased in saturation. Shorting  $V_{in}$  and  $V_{out}$ , a replica bias is readily available [9].

Several low-voltage circuits can be implemented using the body terminal of a MOSFET as an additional

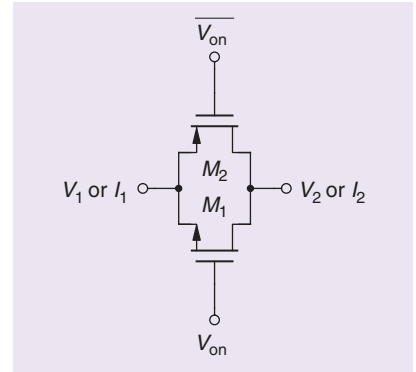


**FIGURE 14:** The transmission gate switches between  $V_1/I_1$  and  $V_2/I_2$  for both voltage and current (and it works rail to rail, too).

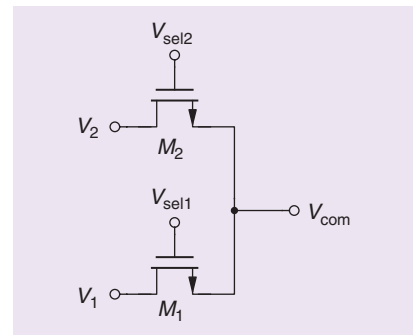


**FIGURE 15:** The two-to-one multiplexer connecting either  $V_1$  or  $V_2$  to  $V_{com}$ . Depending on  $V_{sel1}$  and  $V_{sel2}$ , the MOSFETs are alternately switched on or off.

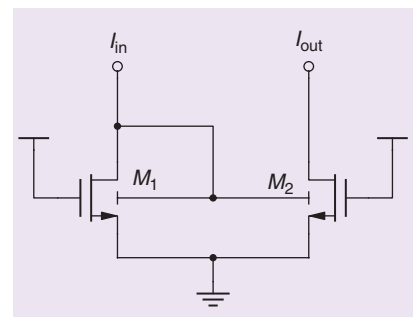
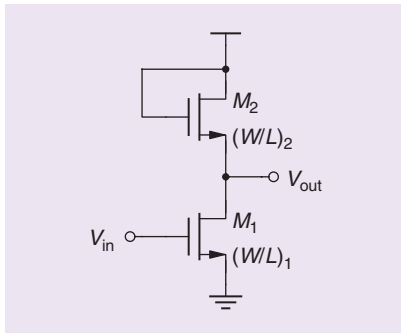


**FIGURE 16:** This circuit is an improved version of Figure 7 in that it allows a low-voltage operation of the current mirror, requiring a voltage headroom substantially less than  $V_{GS1}$  [12].

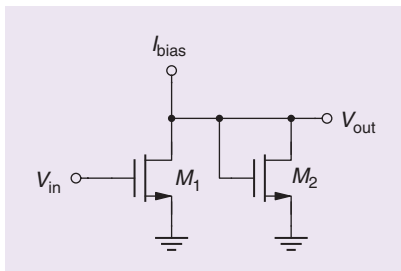
control input, like the low-voltage current mirror depicted in Figure 16. Some arrangements allow for precise voltage-gain and high-speed operation, as demonstrated by the circuits displayed in Figures 17 and 18.

Figure 19 presents an enhanced version of the source follower, also known as a *class-B (push/pull) amplifier*. Degeneration is a primary method to improve matching, noise figure, or output resistance. Different MOSFET-only implementations are feasible (Figures 20 and 21), with the implementation in Figure 21 allowing the performance to be tuned during operation by varying  $V_{bias}$ .

Combining a common-source stage with a common-gate topology [10], as illustrated in Figure 22, results in a differential-output transconductance stage with a single-ended low-ohmic input. It can thus be used under impedance-matched conditions, also providing some noise and linearity



**FIGURE 17:** The common-source amplifier with diode load is sometimes called a *wide-band amplifier* due to its potentially high-speed operation. Here, the gain is set precisely at  $A_v = V_{out}/V_{in} = -\sqrt{(W/L)_1/(W/L)_2}$ , depending only on the transistor sizing (and neglecting the body effect).



**FIGURE 18:** The folded version of Figure 17, which has the advantages of a removed body effect in  $M_2$  and a ground-referred output node [13].

## Some arrangements allow for precise voltage-gain and high-speed operation.

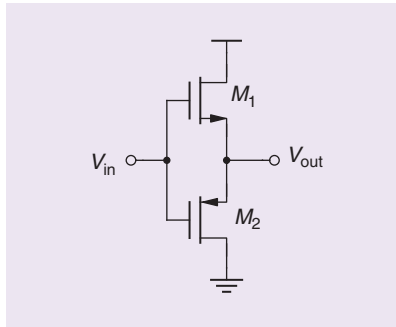


**FIGURE 19:** The class-B push-pull follower can be considered an enhanced version of the simple source follower presented in Figure 9. Lacking a class-A bias component, this structure is subjected to crossover distortion.

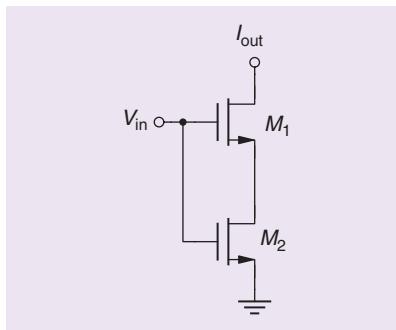


**FIGURE 20:** The MOSFET-R degenerated common-source stage. By appropriately sizing  $M_2$ , the degeneration can be adapted [13]. This arrangement using two transistors can also increase the length of a (compound) device (for example, in current mirrors) as, otherwise, a MOSFET with different  $L$  will not match well.

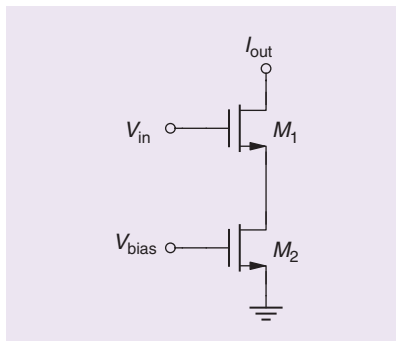


**FIGURE 21:** A variation of the implementation displayed in Figure 20, where the degeneration of  $M_1$  can be adapted by tuning  $V_{bias}$ .

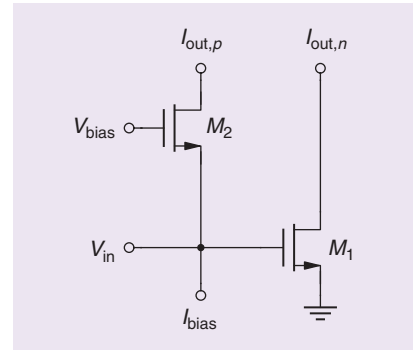


**FIGURE 22:** A common-gate, common-source topology offering impedance-matched, single-ended input and differential output while simultaneously canceling noise and distortion [11].

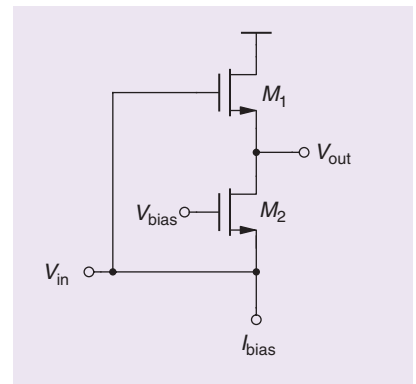


**FIGURE 23:** This low-noise amplifier was discovered by using an exhaustive search of potential two-transistor, wide-band amplifiers. For practical implementation,  $M_1$  requires an ac coupling (and proper biasing) in its gate connection to keep  $M_2$  in saturation [2].

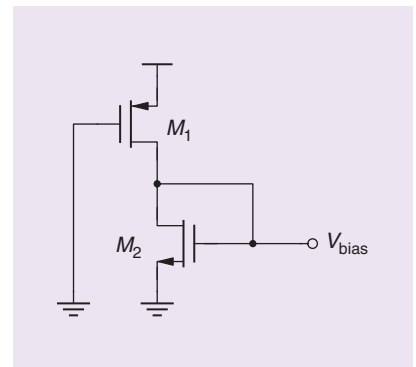


**FIGURE 24:** A (simple) bias-voltage generator using the current source  $M_1$  to bias  $M_2$  so that  $V_{bias} = V_{GS2}$ .

cancellation under the ideal bias [11]. In yet another twist, a source follower can be combined with a common-gate

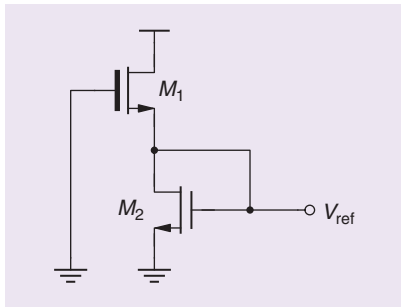


**FIGURE 25:** A constant bias-voltage generator ( $M_1$  and  $M_2$  must have different threshold voltages  $V_{th1} \neq V_{th2}$ ) [14].

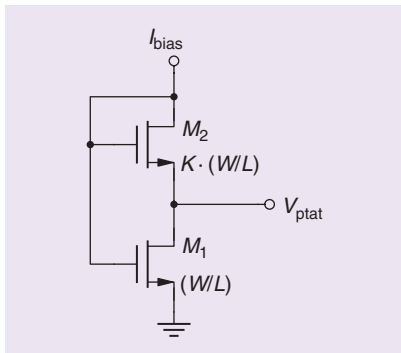


**FIGURE 26:** A proportional-to-absolute-temperature (PTAT) voltage generator if  $M_1$  and  $M_2$  are kept in subthreshold operation [15].

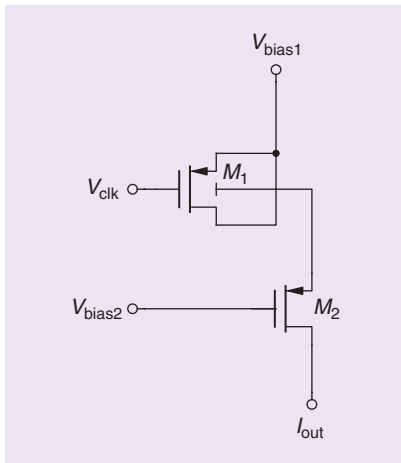


**FIGURE 27:** This pA current source is based on the periodic filling and flushing of Si-SiO<sub>2</sub> interface traps by alternating  $M_1$  between accumulation and inversion (through the proper choice of  $V_{bias1}$  and  $V_{bias2}$  and the switching levels of  $V_{clk}$ ). It can operate with reasonably high clock frequencies and still create tiny currents [16].

stage, resulting in a useful amplifier configuration (see Figure 23), which has been found by systematically generating graphs consisting of two trans-conductance stages [2].

### Biasing Circuits

The generation of a bias voltage is a task that is often encountered in analog circuit design. When the requirements on stability are moderate, a simple configuration, as displayed in Figure 24, might be sufficient. A surprisingly stable voltage reference can be constructed from two MOSFETs with different threshold voltages, as demonstrated in Figure 25. Occasionally, a bias voltage with a well-defined proportionality to temperature is needed, for example, in temperature-sensor circuits. This effect can be achieved by a PTAT voltage generator like the one depicted in Figure 26. Sometimes, circuits

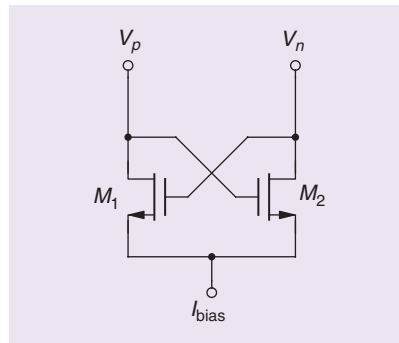


**FIGURE 28:** Two transistors with cross-coupling form a negative resistance between  $V_p$  and  $V_n$  and are mainly employed in oscillators and comparators. As in Figure 8, the bias-current source can be replaced by a fixed potential.

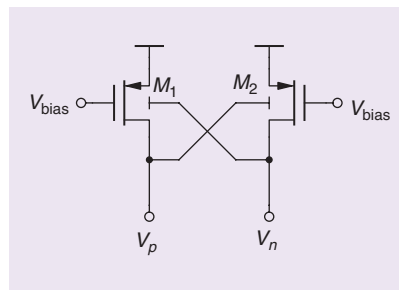


**FIGURE 29:** This circuit is a low-voltage version of Figure 28, where the body controls the MOSFET, avoiding the significant  $V_{GS}$  drop at  $V_p$  and  $V_n$  [18].

are based on obscure second-order effects, like charge trapping in the Si-SiO<sub>2</sub> interface traps, which are used in the clocked circuit displayed in Figure 27 and can create pA-currents in an area-efficient manner.

### Diverse Circuit Elements

The various operating modes of a MOSFET can be utilized differently and lead to practical circuit elements. The cross-coupled differential pair (see Figures 28 and 29) synthesizes a negative resistance, which can cancel losses, for example, in oscillators

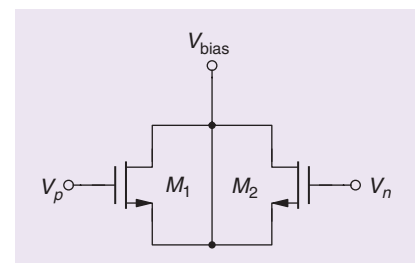


**FIGURE 30:** The varactor (the capacitance between  $V_p$  and  $V_n$  depends on the bias voltage  $V_{bias}$ ) is often used in voltage-controlled oscillators. In most technologies, the NMOS can be put inside the n-well so that the varactor works in accumulation, providing an optimized tuning range and high  $Q$  [19].

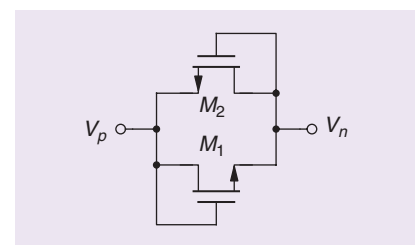


**FIGURE 31:** The antiparallel diodes can be employed for many things, for example, voltage clamping.

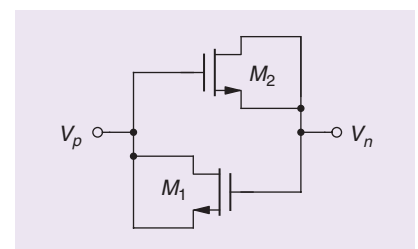


**FIGURE 32:** The antiparallel MOSFET capacitors make the differential capacitance more linear and symmetrical. As in Figure 30, an NMOS in n-well is an option.

or  $Q$ -enhanced  $LC$  filters. Since the effective capacitance between the gate terminal and the source/drain connection of a MOSFET is a function of biasing conditions, the arrangement demonstrated in Figure 30 can be employed as a varactor.

Using local feedback to create a MOSFET “diode,” two antiparallel diodes can replace conventional  $pn$ -diodes, for example, in voltage limiters (Figure 31). The gate oxide of a MOSFET usually offers the highest capacitance density in a given CMOS technology, so an antiparallel pair of MOSFETs (see Figure 32) can substitute a linear capacitor with one that has mediocre linearity but is much smaller. This structure has the additional benefit of symmetrical parasitic capacitors at both terminals.

## A surprisingly stable voltage reference can be constructed from two MOSFETs with different threshold voltages.

An active inductor can be simulated by transistors using gyrator principles [17], offering a significant area reduction compared to what’s offered by a passive implementation based on a coil constructed from the metal layers. An exemplary implementation based on two MOSFETs is displayed in Figure 33.

### Analog Signal Processing

The processing of analog signals is often needed when devising circuits. The area-efficient division of voltages (see Figure 34) or currents [either employing a current mirror

(as in Figure 7) or the advanced usage of the Bult current divider (presented in Figure 35)] can become handy. In most implementations of an analog-to-digital converter, a sample-and-hold stage is required, which often exploits the excellent switching capabilities of the MOSFET, as demonstrated in Figure 36, where a MOSFET configured as a capacitor stores the sampled voltage. Sampling can be used for frequency conversion, which can also be achieved through the arrangement in Figure 37, where the time-variant

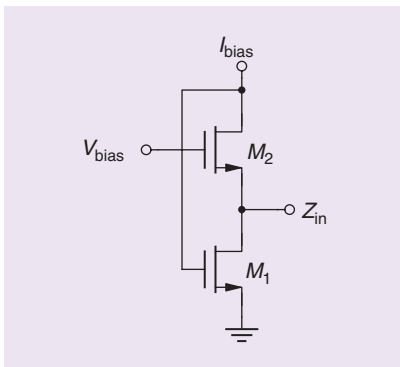


**FIGURE 33:** This circuit, which is a similar configuration of the flipped voltage follower in Figure 47, can function as an active inductor, providing  $L = C_{GS1}/(g_{m1} \cdot g_{m2})$  [20].

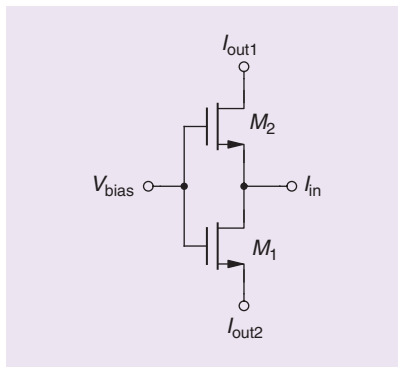


**FIGURE 35:** The Bult current divider (if  $M_1$  and  $M_2$  are of identical size, then  $I_{in}$  is precisely split in half between  $I_{out1}$  and  $I_{out2}$ ) [22].

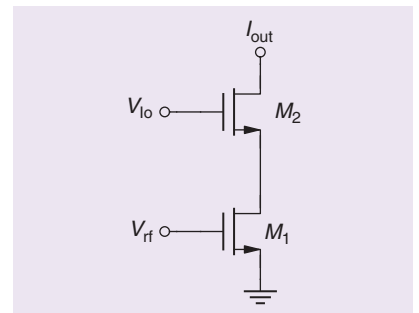


**FIGURE 37:** In the dual-gate MOSFET (a similar arrangement as in Figure 11), the periodic local-oscillator signal  $V_{io}$  causes the time-variant change of the transconductance of  $M_1$ , resulting in a frequency conversion from the input  $V_{rf}$  to the output  $I_{out}$  [21].

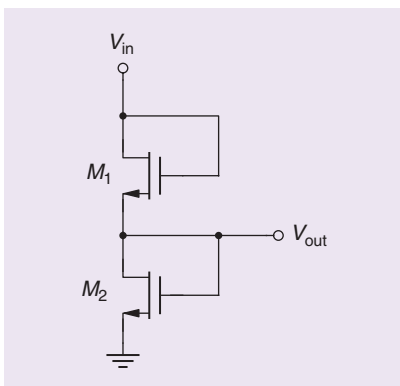


**FIGURE 34:** An area-efficient voltage divider. If  $M_1$  and  $M_2$  are the same size, then  $V_{out} \approx V_{in}/2$ . Often, a PMOS version is a better choice since it can avoid the body effect by tying the body to the respective source for  $M_1$  and  $M_2$ .

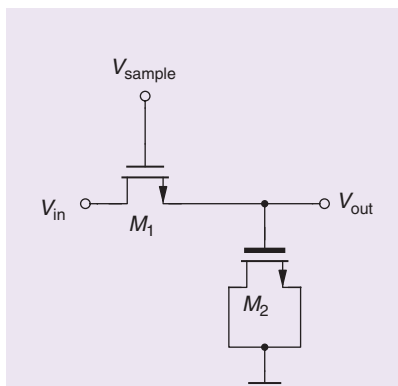


**FIGURE 36:** A sample-and-hold circuit implementing the gate capacitance of  $M_2$  as a storage capacitor (a low to zero  $V_{th}$  would be an advantage in this case) [23].

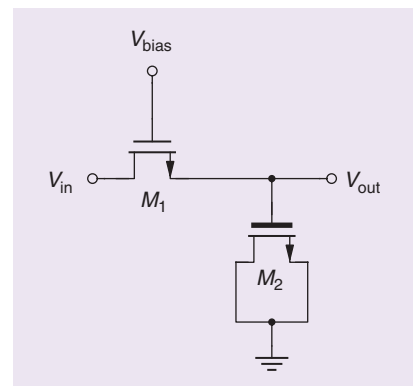


**FIGURE 38:** The circuit of Figure 36 becomes a continuous-time, low-pass filter if  $M_1$  gets a fixed bias instead of a clock signal. Note that this circuit transforms into a high-pass filter when  $M_1$  and  $M_2$  are swapped.

## Circuits working with the body terminal as a fourth control input can add many possibilities.

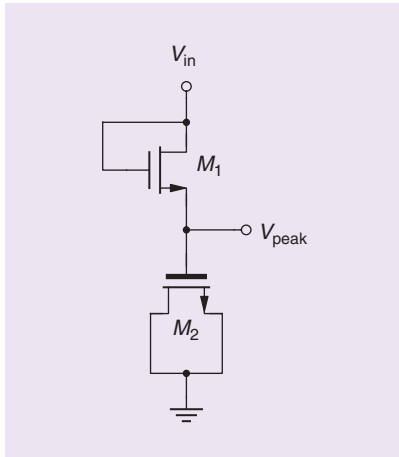


**FIGURE 39:** A voltage-peak detector, where  $V_{\text{peak}} = V_{\text{in,max}} - V_{\text{gs1}}$ .

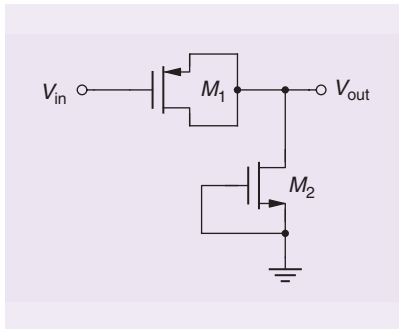


**FIGURE 40:** A similar circuit to Figure 39, which can function as an approximate voltage doubler when driven by a sinusoidal input voltage. On negative swings of  $V_{\text{in}}$ , the capacitor  $M_1$  gets charged to  $|V_{\text{in}}| - V_{\text{gs2}}$ , which is added to  $V_{\text{in}}$  during positive swings when  $M_2$  is off. As with any circuit with negative voltages, proper connection of the wells is required [24].

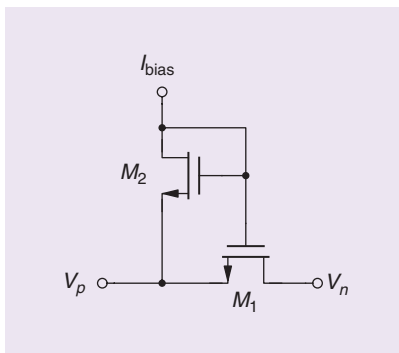


**FIGURE 41:** The controlled (high-impedance) floating resistor.

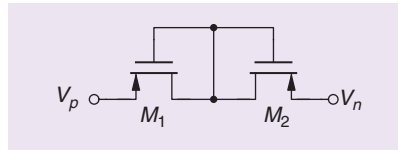


**FIGURE 42:** This arrangement creates an enormous resistance between  $V_p$  and  $V_n$ , although it is also susceptible to temperature and process variations [25].

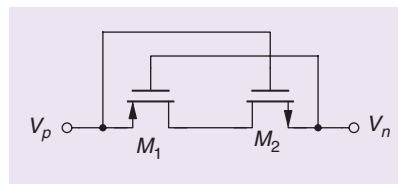


**FIGURE 43:** The ultralow-power diode (ULPD) with reduced leakage in the reverse direction [26].

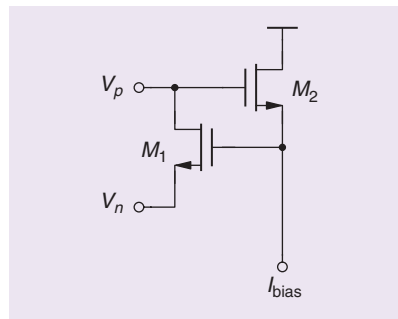


**FIGURE 44:** The floating level shift (or “floating battery”) effectively shifts a bias point between  $V_p$  and  $V_n$  as  $V_{\text{shift}} = V_p - V_n = V_{\text{GS1}} + V_{\text{GS2}}$ .

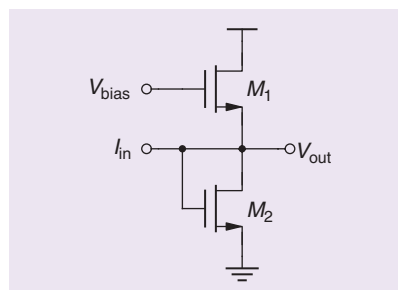


**FIGURE 45:** This circuit is a perfectly linear  $I$ -to- $V$  converter with  $V_{\text{out}}/I_{\text{in}} = [\mu C_{\text{ox}} \cdot (W/L) \cdot (V_{\text{bias}} - 2V_{\text{th}})]^{-1}$  if we assume a square-law behavior, and  $M_1$  and  $M_2$  are the same size and kept in saturation (and neglecting body effect) [27].

change of the transconductance of  $M_1$  causes a mixing effect [21].

Realizing the MOSFET operating as a controlled resistor in the triode region, Figure 36 can be easily transformed into a (programmable) low-pass filter, as illustrated in Figure 38. By rewiring the sampling switch into the diode-equivalent MOSFET configuration, a voltage-peak detector (Figure 39) and an approximate voltage doubler (Figure 40) can be built for ac signals.

### Simple Circuits With a Twist

While most CMOS processes provide thin-film resistors, it is often difficult to realize values in the  $M\Omega$  to  $G\Omega$  range. The MOSFET in triode or off-state (Figures 41 and 42) is a good alternative at a much smaller silicon area. An improved version of a diode-connected MOSFET is demonstrated in Figure 43. This two-transistor construction, called the

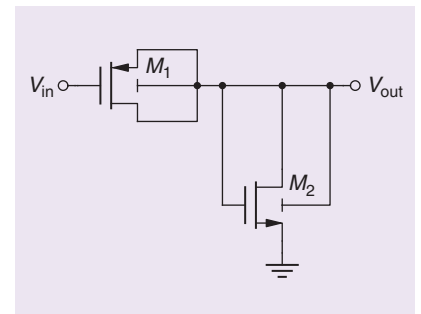


**FIGURE 46:** This circuit shifts a digital input voltage  $V_{\text{in}}$  to an output voltage  $V_{\text{out}}$  swinging around  $V_{\text{SS}}$  [28].

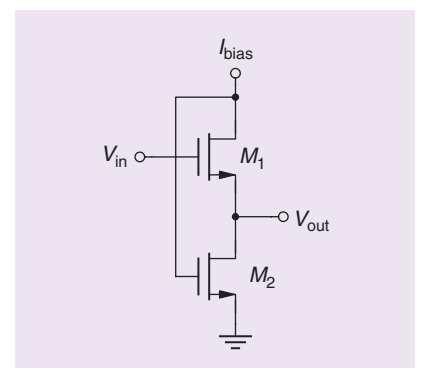


**FIGURE 47:** The flipped voltage follower is an improved version of Figure 9, employing feedback to lower the output impedance to  $r_{\text{out}} = g_{\text{ds2}}/(g_{\text{m1}} \cdot g_{\text{m2}})$  [29].

ULPD, considerably lowers the leakage current in the reverse direction. A level shift is often needed in a signal path, which can be imple-

## Compensating for the low $\beta$ of the parasitic BJT can be achieved by implementing the structure depicted in Figure 50.

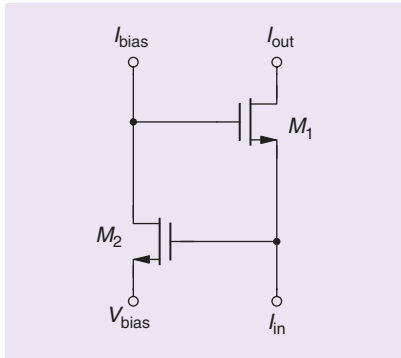


**FIGURE 48:** The regulated cascode increasing the effect of the cascode  $M_1$  by  $g_{m2}/g_{ds2}$  due to feedback. Note that the source of  $M_2$  can be tied to the ground if combined with a common-source input stage [30].

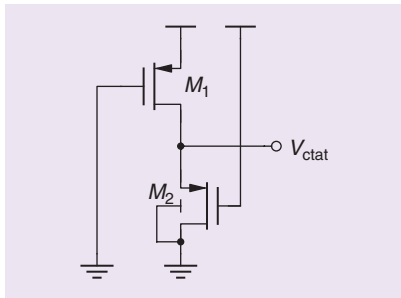


**FIGURE 49:** This simple CTAT voltage generator can be created by exploiting the parasitic (lateral or vertical) PNP transistor inherent in a PMOS structure [31].

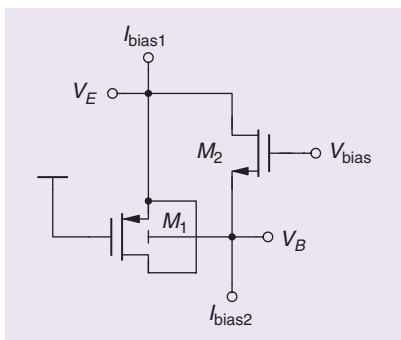


**FIGURE 50:** The parasitic BJT introduced in Figure 49 often suffers from poor  $\beta$ . This circuit forces the collector current of the parasitic (vertical) p-n-p to  $I_C = I_{bias1} - I_{bias2}$ , although the collector terminal (being the p-substrate) is not accessible. By doing this, the resulting  $V_{EB} = V_E - V_B$  can be accurately employed in a bandgap circuit [32].

mented as pictured in Figure 44. Sometimes a simple circuit shows a surprising property, and the linear  $I$ -to- $V$  converter illustrated in Figure 45 is such an example.

Circuits working with the body terminal as a fourth control input can add many possibilities, like the logic-level shift implemented in Figure 46. Feedback is an essential tool in a circuit designer's box: The flipped voltage follower (displayed in Figure 47) and the regulated cascode (see Figure 48) are significantly improved versions of their simpler counterparts presented in Figures 9 and 12, respectively.

### Using the MOSFET as a BJT

Inherent to the physical structure of a MOSFET is a bipolar junction transistor (BJT), which often shows inadequate performance, like poor current gain  $\beta \ll 10$ . Still, it can be employed to generate a temperature-dependent voltage, like the circuit presented in Figure 49, whose proportional-to-complementary-temperature (CTAT) property is an excellent addition to the PTAT behavior of the circuit in Figure 26. Compensating for the low  $\beta$  of the parasitic BJT can be achieved by implementing the structure depicted in Figure 50, which improves the accuracy of a bandgap circuit built from these augmented BJT devices.

### Conclusions

Fifty practical circuit snippets employing just two MOS transistors have been presented. The motivation behind this compilation is to celebrate the creativity in analog circuit design and to demonstrate the versatility of the fabulous MOSFET. Walking through these examples (and considering that this compendium is far from complete [3]) leaves one in awe as one thinks about the endless possibilities that are gen-

erated when an analog circuit designer is given a handful of these fantastic transistors.

### Acknowledgments

We thank the reviewers for their many mindful suggestions. We want to thank our colleagues at the Institute for Integrated Circuits, Johannes Kepler University Linz, for their support in preparing this manuscript and for their many enlightening discussions.

### References

- [1] E. A. M. Klumperink, F. Bruccoleri, and B. Nauta, "Finding all elementary circuits exploiting transconductance," *IEEE Trans. Circuits Syst. II, Exp. Briefs*, vol. 48, no. 11, pp. 1039–1053, 2001. doi: 10.1109/82.982356.
- [2] F. Bruccoleri, E. A. M. Klumperink, and B. Nauta, "Generating all two-MOS-transistor amplifiers leads to new wide-band LNAs," *IEEE J. Solid-State Circuits*, vol. 36, no. 7, pp. 1032–1040, 2001. doi: 10.1109/4.933458.
- [3] D. Shahhosseini, E. Zailer, L. Behjat, and L. Belostotski, "Method of generating unique elementary circuit topologies," *Can. J. Elect. Comput. Eng.*, vol. 41, no. 3, pp. 118–132, 2018. doi: 10.1109/CJCE.2018.2859621.
- [4] F. Wanlass and C. Sah, "Nanowatt logic using field-effect metal-oxide semiconductor triodes," in *Proc. IEEE ISSCC Dig. Tech. Papers*, 1963, pp. 32–33. doi: 10.1109/ISSCC.1963.1157450.
- [5] F. Assaderaghi, S. Parke, D. Sinitysky, J. Bokor, P. K. Ko, and C. Hu, "A dynamic threshold voltage MOSFET (DTMOS) for very low voltage operation," *IEEE Electron Device Lett.*, vol. 15, no. 12, pp. 510–512, 1994. doi: 10.1109/55.338420.
- [6] D. E. Fulkerson, "Direct-coupled transistor-transistor logic: new high-performance LSI gate family," *IEEE J. Solid-State Circuits*, vol. 10, no. 2, pp. 110–117, 1975. doi: 10.1109/JSSC.1975.1050570.
- [7] R. Widlar, "Some circuit design techniques for linear integrated circuits," *IEEE Trans. Circuit Theory*, vol. 12, no. 4, pp. 586–590, 1965. doi: 10.1109/TCT.1965.1082512.
- [8] A. D. Blumlein, "Thermionic valve amplifying circuit," U.S. Patent 2 185 367, 1937.
- [9] B. Nauta and E. Seevinck, "Linear CMOS transconductance element for VHF filters," *Electron. Lett.*, vol. 25, no. 7, pp. 448–450, Mar. 1989. doi: 10.1049/el:19890308.
- [10] B. Nauta, "Single-to-differential converter," U.S. Patent 5 404 050, Apr. 4, 1995.
- [11] S. C. Blaauwmeier, E. A. M. Klumperink, D. M. W. Leenaerts, and B. Nauta, "Wideband balun-LNA with simultaneous output balancing, noise-canceling and distortion-canceling," *IEEE J. Solid-State Circuits*, vol. 43, no. 6, pp. 1341–1350, 2008. doi: 10.1109/JSSC.2008.922736.

- [12] B. J. Blalock and P. E. Allen, "A low-voltage, bulk-driven MOSFET current mirror for CMOS technology," in *Proc. IEEE Int. Symp. Circuits Syst. (ISCAS)*, 1995, pp. 1972–1975.
- [13] W. Sansen, *Analog Design Essentials*. New York: Springer-Verlag, 2006. doi: 10.1109/ISCAS.1995.523807.
- [14] M. Seok, G. Kim, D. Blaauw, and D. Sylvester, "A portable 2-transistor picowatt temperature-compensated voltage reference operating at 0.5 V," *IEEE J. Solid-State Circuits*, vol. 47, no. 10, pp. 2534–2545, 2012. doi: 10.1109/JSSC.2012.2206683.
- [15] A. Amaravati, M. Dave, M. S. Baghini, and D. K. Sharma, "800-nA process-and-voltage-invariant 106-dB PSRR PTAT current reference," *IEEE Trans. Circuits Syst. II, Exp. Briefs*, vol. 60, no. 9, pp. 577–581, 2013. doi: 10.1109/TCSII.2013.2268435.
- [16] U. Cilingiroglu, A. Becker-Gomez, and K. T. Veeder, "An evaluation of MOS interface-trap charge pump as an ultralow constant-current generator," *IEEE J. Solid-State Circuits*, vol. 38, no. 1, pp. 71–83, 2003. doi: 10.1109/JSSC.2002.806282.
- [17] D. Qiu, "Circuit design of an integrable simulated inductor and its applications," *IEEE Trans. Instrum. Meas.*, vol. 40, no. 6, pp. 902–907, 1991. doi: 10.1109/19.119765.
- [18] S. Chatterjee, Y. Tividis, and P. Kinget, "0.5-V analog circuit techniques and their application in OTA and filter design," *IEEE J. Solid-State Circuits*, vol. 40, no. 12, pp. 2373–2387, 2005. doi: 10.1109/JSSC.2005.856280.
- [19] T. Soorapanth, C. P. Yue, D. K. Shafer, T. I. Lee, and S. S. Wong, "Analysis and optimization of accumulation-mode varactor for RF ICs," in *Proc. Symp. VLSI Circuits*, 1998, pp. 32–33. doi: 10.1109/VLSI.1998.687993.
- [20] Y. Wu, M. Ismail, and H. Olsson, "A novel CMOS fully differential inductorless RF bandpass filter," in *Proc. IEEE Int. Symp. Circuits Syst. (ISCAS)*, 2000, pp. 149–152. doi: 10.1109/ISCAS.2000.858710.
- [21] S. C. Cripps, O. Nielsen, D. Parker, and J. A. Turner, "An experimental evaluation of X-band mixers using dual-gate GaAs MESFETs," in *Proc. 1977 7th Eur. Microw. Conf.*, pp. 101–104. doi: 10.1109/EUMA.1977.332410.
- [22] K. Bult and G. J. G. M. Geelen, "An inherently linear and compact MOST-only current division technique," *IEEE J. Solid-State Circuits*, vol. 27, no. 12, pp. 1730–1735, 1992. doi: 10.1109/4.173099.
- [23] R. Mao, K. Keller, and R. Ahrons, "Integrated MOS analog delay line," in *IEEE ISSCC Dig. Tech. Papers*, 1969, pp. 164–165. doi: 10.1109/JSSC.1969.1049996.
- [24] P. Villard, "Transformateur à haut voltage. A survolteur cathodique," *J. Phys. Theor. Appl.*, vol. 10, no. 1, pp. 28–32, 1901. doi: 10.1051/jphys:019010010002801.
- [25] R. R. Harrison, "A low-power, low-noise CMOS amplifier for neural recording applications," in *Proc. IEEE Int. Symp. Circuits Syst. (ISCAS)*, 2002, pp. 197–200. doi: 10.1109/ISCAS.2002.1010674.
- [26] D. Levacq, C. Liber, V. Dessard, and D. Flandre, "Composite ULP diode fabrication, modelling and applications in multi-Vth FD SOI CMOS technology," *Solid-State Electron.*, vol. 48, no. 6, pp. 1017–1025, 2004. doi: 10.1016/j.sse.2003.12.016.
- [27] K. Bult and H. Wallinga, "A class of analog CMOS circuits based on the square-law characteristic of an MOS transistor in saturation," *IEEE J. Solid-State Circuits*, vol. 22, no. 3, pp. 357–365, 1987. doi: 10.1109/JSSC.1987.1052733.
- [28] H-Y Huang and J-F Lin, "CMOS bulk input technique," in *Proc. IEEE Int. Symp. Circuits Syst. (ISCAS)*, 2002, p. III. doi: 10.1109/ISCAS.2002.1010208.
- [29] J. Ramirez-Angulo, R. G. Carvajal, A. Torralba, J. Galan, A. P. Vega-Leal, and J. Tombs, "The flipped voltage follower: A useful cell for low-voltage low-power circuit design," in *Proc. IEEE Int. Symp. Circuits Syst. (ISCAS)*, 2002, p. III. doi: 10.1109/ISCAS.2002.1010299.
- [30] B. J. Hosticka, "Improvement of the gain of MOS amplifiers," *IEEE J. Solid-State Circuits*, vol. 14, no. 6, pp. 1111–1114, 1979. doi: 10.1109/JSSC.1979.1051324.
- [31] E. A. Vittoz, "MOS transistors operated in the lateral bipolar mode and their application in CMOS technology," *IEEE J. Solid-State Circuits*, vol. 18, no. 3, pp. 273–279, 1983. doi: 10.1109/JSSC.1983.1051939.
- [32] M. Eberlein, "Bandgap reference circuit with beta-compensation," U.S. Patent 9 568 929 B2, Feb. 14, 2017.

## About the Authors

**Harald Pretl** (harald.pretl@jku.at) received his Dipl. Ing. degree in electrical engineering from TU Graz, Austria, in 1997, and his Dr.techn. degree from the Johannes Kepler University Linz (JKU) in Linz, Austria,

in 2001. From 2000 to 2011, Pretl worked at Infineon Technologies as director and senior principal engineer; from 2011 to 2019, he worked at Intel as senior principal engineer. Since 2015, he has been a full professor at the Institute for Integrated Circuits at JKU, Linz, 4040, Austria, heading the Energy-Efficient Analog Circuits and Systems group. His current research interests are radio-frequency transceivers, mobile communications and the Internet of Things, sensors, and micropower systems on chip. He is a Senior Member of IEEE.

**Matthias Eberlein** (matthias.eberlein@jku.at) received his German Diplom degree in semiconductor electronics from the TU Darmstadt, Germany, in 1995. He started his career as an analog-design engineer for transceiver systems on chips with Infineon in Munich. Later, he had various assignments in Germany and Asia and, most recently, worked for Intel and Apple corporations. In parallel, he studied at the Johannes Kepler University Linz, 4040, Linz, Austria, toward a Ph.D. degree in thermal sensor topics. Eberlein has authored about 30 patents and was the recipient of the first IEEE Brockaw Award for Circuit Elegance in 2020. His current research interests include low-power, sensor, and reference circuits in FinFET technologies. He is a Member of IEEE.

SSC